

**THE SABRELINER DATA SET OF THE FIRE
CIRRUS IFO FIRE SERIES No. 1**

by

Paul F. Hein, Stephen K. Cox and
Christopher Johnson-Pasqua

Department of Atmospheric Science
Colorado State University
Fort Collins, Colorado



**Department of
Atmospheric Science**

Paper No. 418

The Sabreliner Data Set of the FIRE Cirrus IFO

FIRE Series No. 1

by

Paul F. Hein,

Stephen K. Cox

and

Christopher Johnson-Pasqua

Department of Atmospheric Science

Colorado State University

Fort Collins, CO 80523

November, 1987

Atmospheric Science Paper No. 418

ACKNOWLEDGEMENTS

The authors wish to thank Paul Stackhouse, Jr. and William Smith, Jr. for the information they supplied on the bug-eye calibration and radiometer temperature sensitivities, respectively. This research was funded by the National Science Foundation under grant ATM-8521214 and the National Aeronautics and Space Administration under grant NAG 1-554. The Sabreliner aircraft was provided by the National Center for Atmospheric Research (NCAR) Research Aviation Facility and computer support was furnished by the NCAR Scientific Computing Division. NCAR is supported by the National Science Foundation.

TABLE OF CONTENTS

	<u>Page</u>
ACKNOWLEDGEMENTS	ii
TABLE OF CONTENTS	iii
LIST OF TABLES	iv
LIST OF FIGURES	v
1.0 INTRODUCTION	1
2.0 INSTRUMENTATION	4
2.1 NCAR Instrumentation	4
2.2 CSU Instrumentation	10
3.0 DATA DESCRIPTION	15
3.1 Data Accessible from the CSU Vax Computer	15
3.2 Data Archived on Streaming Tape	20
3.3 Data Quality	23
REFERENCES	27
APPENDIX 1: SABRELINER FLIGHT SUMMARIES	28
APPENDIX 2: SABRELINER FLIGHT LEG TIMES	35
APPENDIX 3: SHORT DESCRIPTION OF AVAILABLE PROGRAMS	44

LIST OF TABLES

	<u>Page</u>
Table 1. VHS Video Camera Log.	5
Table 2a. Coefficients of pyranometer correction equation 1a for $T_S < T_{S1}$.	9
Table 2b. Coefficients of pyranometer correction equation 1b for $T_S \geq T_{S1}$.	9
Table 3. The angular positions of the bugeye photodiodes.	12
Table 4. Bugeye zero offsets and ratios of Photodiode 1 to Photodiode i.	12
Table 5. Files of the Vax labeled tapes.	16
Table 6. The variables on Vax tape.	17
Table 7. Streaming tape variables in order of appearance on tape.	21

LIST OF FIGURES

	<u>Page</u>
Figure 1. Relative sensitivities of two pyranometers and a pyrgeometer to temperature.	8
Figure 2. Spectral response of the Bugeye photodiodes.	13

1.0 INTRODUCTION

This paper provides a summary of information used in processing the Sabreliner aircraft data collected during the Cirrus Intensive Field Observations (Cirrus IFO) of the First ISCCP (International Satellite Cloud Climate Program) Regional Experiment (FIRE). Emphasis is placed on the processing of the Colorado State University (CSU) data products.

The Cirrus IFO of FIRE was conducted in Wisconsin from 13 October 1986 to 02 November 1986. The FIRE experiment was designed to emphasize the simultaneous collection of data from multiple platforms. Aircraft flights were usually conducted at times of satellite overpasses and over ground stations containing radiation instrumentation and lidar. Extra rawinsondes were released in the area with launches every three hours on selected days. Three research aircraft based out of Madison, Wisconsin flew during the experiment: the NCAR Sabreliner, NCAR King Air, and the NASA ER-2. The NASA ER-2 was flown at very high altitudes (about 17 km) and was used to map the cirrus from above and to simulate a satellite. The King Air and Sabreliner were deployed to make detailed microphysical and radiometric measurements along with the basic atmospheric state observations. The King Air was usually deployed below 30,000 feet with the Sabreliner above 30,000 feet.

The objectives of the FIRE Cirrus IFO as stated by Starr (1987) are:

- "1) To characterize the bulk physical structure of cirrus cloud fields, the associated radiative fields and the corresponding large-scale meteorological environment. The cloud properties of interest are the vertically integrated ice-water path (IWP), and broadband and 'window' radiative properties. Description of the radiative fields will include the broadband radiative fluxes as well as the directionally and spectrally dependent radiance fields;
- 2) To characterize the fine-scale microphysical, radiative, thermodynamic, and dynamic structure of the cirrus clouds at various stages of their life cycles and the concomitant environmental conditions. Here, the cloud properties of interest also specifically include the ice-water-content, (and liquid if present), cloud-particle size distribution and ice crystal habit;
- 3) To characterize relationships between cloud properties inferred from satellite observations at various scales to those obtained directly or inferred from very high-resolution measurements."

Section 2 will give a brief description of the instrumentation aboard the Sabreliner and Section 3 will

describe the data and data products. Appendix 1 gives a brief description of each of the flights. A table of flight leg start and end times is found in Appendix 2, and a description of some of the programs available on the PC is given in Appendix 3.

2.0 INSTRUMENTATION

2.1 NCAR Instrumentation

The NCAR instrumentation measured aircraft position, aircraft velocity, aircraft altitude, static pressure, dynamic pressure, temperature, dew point temperature, humidity, air flow, icing, cloud and precipitation particle size, visible radiation and infrared radiation. Two video cameras, one looking forward and the other looking out the right side, recorded the flights. Table 1 contains a catalog the video cassettes.

Radiometric Instrumentation

Aboard the Sabreliner was four Research Aviation Facility (RAF) Modified Eppley Model PSP Pyranometers and two RAF Modified Eppley Model PIR Pyrgeometers. Two of the pyranometers (SWT1 and SWB1) had clear domes and a spectral range from .3 to 3 microns. The other two pyranometers (SWT2 and SWB2) had red domes with a spectral range from .7 to 3 microns.

Two of the pyranometers (SWT1 and SWT2) and a pyrgeometer (IRB) were tested for calibration sensitivity to temperature from -70°C to 26°C. The results of the testing are found in Figure 1. The data has been normalized with the 26°C value, since Eppley calibrated the pyranometers at 25°C. A large drop in sensitivity is seen at the colder

Table 1. VHS Video Camera Log.

Flt. No.	Julian Day	1986 Date	Camera Location	C.U.T. Start Time	C.U.T. Stop Time	Remarks
R-1	286	13 Oct	Forward	182725	193400	
R-1	286	13 Oct	Left Side	182725	193400	
R-2	288	15 Oct	Forward	181000	204820	
R-2	288	15 Oct	Left Side	181000	204820	
R-3	292	19 Oct	Forward	150710	175734	
R-3	292	19 Oct	Left Side	150710	175734	
R-4	292	19 Oct	Forward	193507	222617	
R-4	292	19 Oct	Left Side	193507	222617	
R-5	293	20 Oct	Forward	141345	163620	
R-5	293	20 Oct	Left Side	141345	163620	
R-6	294	21 Oct	Forward	164745	193610	
R-6	294	21 Oct	Left Side	164745	193610	
R-7	295	22 Oct	Forward	133140	162500	
R-7	295	22 Oct	Left Side	133140	162500	
R-8	295	22 Oct	Forward	175806	205545	
R-8	295	22 Oct	Left Side	175806	205545	
R-9	297	24 Oct	Forward	180115	205055	
R-9	297	24 Oct	Left Side	180115	205055	
R-10	300	27 Oct	Forward	174500	202600	
R-10	300	27 Oct	Left Side	174500	202600	
R-11	300	27 Oct	Forward	222000	244400	
R-11	300	27 Oct	Left Side	222000	244400	

Table 1. (Continued)

Flt. No.	Julian Day	1986 Date	Camera Location	C.U.T. Start Time	C.U.T. Stop Time	Remarks
R-12	301	28 Oct	Forward	150130	170800	
R-12	301	28 Oct	Left Side	150130	170800	
R-13	301	28 Oct	Forward	185400	214140	
R-13	301	28 Oct	Left Side	185400	214140	
R-14	303	30 Oct	Forward	175015	205220	
R-14	303	30 Oct	Left Side	175015	205220	Time encoding inop after 171832
R-15	304	31 Oct	Forward	140845	165430	
R-15	304	31 Oct	Left Side	140845	165430	
R-16	304	31 Oct	Forward	190900	220450	
R-16	304	31 Oct	Left Side	190900	220450	
R-17	306	2 Nov	Forward	150307	175130	
R-17	306	2 Nov	Left Side	150307	175130	
R-18	306	2 Nov	Forward	192327	215905	
R-18	306	2 Nov	Left Side	192327	215905	

temperatures. Correction curves have been developed to correct the pyranometer data. The pyranometers can be corrected using an adjacent pyrgeometer sink temperature (T_S) and applying the following set of equations in the proper temperature ranges. The coefficients for the equations can be found in Table 2a and Table 2b.

$$A \cdot T_S + B \quad \text{for } T_S < T_{S1} \quad (1a)$$

$$C \cdot T_S^2 + D \cdot T_S + E \quad \text{for } T_S \geq T_{S1} \quad (1b)$$

The serial number of IRB is 12150F3 and for IRT it is 12151F3.

PMS Probes

Two dimensional optical array probes, Particle Measuring Systems Models 2D-C and 2D-P, were used to measure the size of the cloud and precipitation particles. The instruments were mounted below the wing. As described by Baumgardner (1985), the 2-D probes consist of a laser beam that shines through a sampling volume, and a linear array of photodiodes which detects the transmitted beam on the other side of the sampling volume. When a particle passes through the beam in the sampling volume, a shadow appears on the diodes and with consecutive measurements of the photodiode array a two dimensional image is captured. The probes also can determine if the particle is ice or liquid water by the polarization of the scattered laser beam. A tremendous amount of data is collected and this fast data collection rate can, at times of

CSU-NCAR(RAF) 9/87

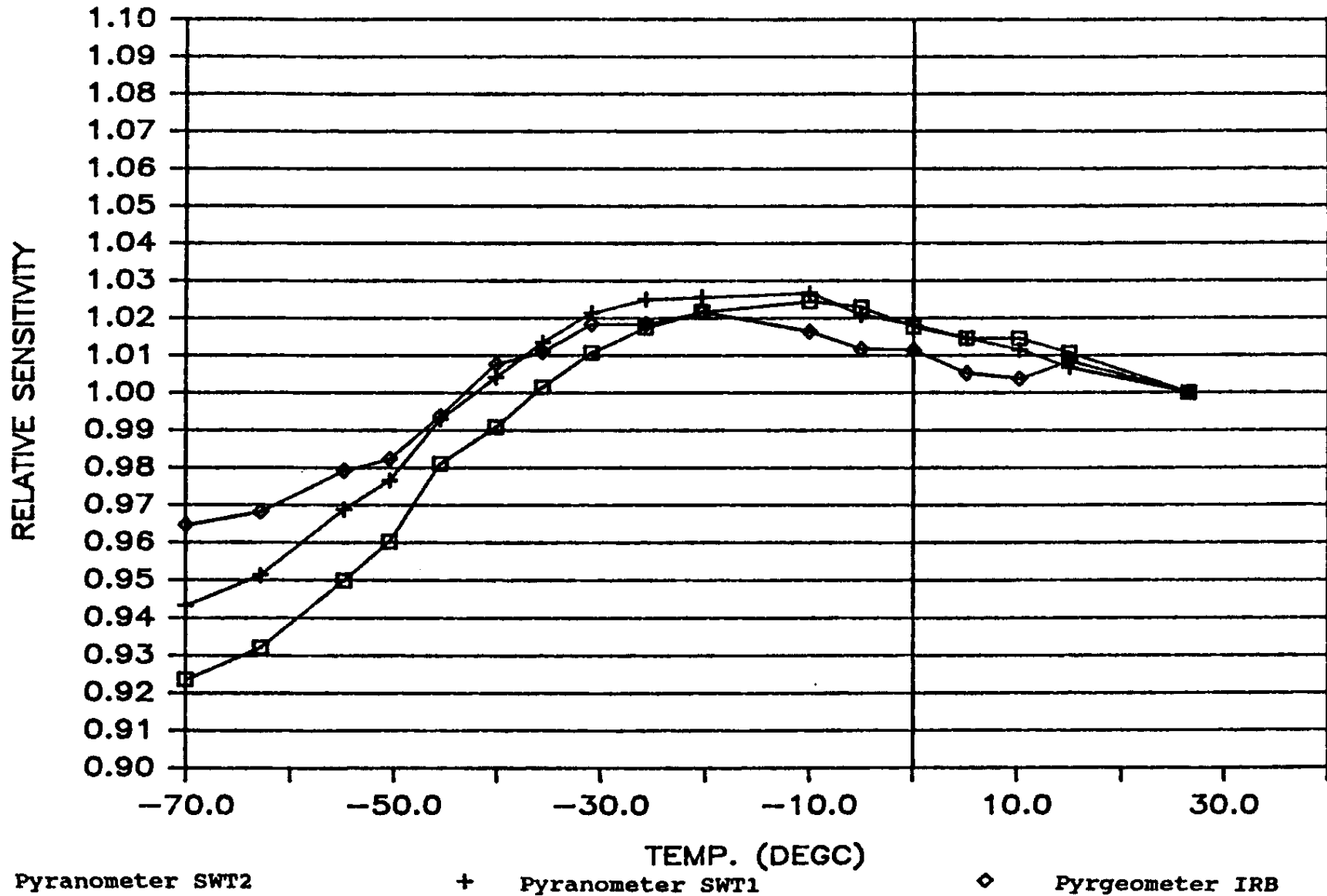


Figure 1. Relative sensitivities of two pyranometers and a pyrgometer to temperature.

Table 2a. Coefficients of pyranometer correction
equation 1a for $T_S < T_{S1}$.

Pyranometer	Serial Number	T_{S1} (°C)	A	B
SWT1	12149F3	-30.165	2.0393E-3	0.52632
SWT2	14963F3	-28.337	2.3174E-3	0.44895
SWB1	12148F3	-29.212	2.1784E-3	0.48763
SWB2	14962F3	-29.212	2.1784E-3	0.48763

Table 2b. Coefficients of pyranometer correction
equation 1b for $T_S \geq T_{S1}$.

Pyranometer	T_{S1} (°C)	C	D	E
SWT1	-30.165	-1.5598E-3	7.9952E-3	5.9432E-5
SWT2	-28.337	-1.4831E-3	7.7818E-3	5.7846E-5
SWB1	-29.212	-1.5214E-3	7.8885E-3	5.8639E-5
SWB2	-29.212	-1.5214E-3	7.8885E-3	5.8639E-5

high particle concentration, cause data to be lost if the data buffer overflows. The PMS 2D-C was set up with a 50 micron resolution and measured particles from 50 to 1600 microns. (The PMS 2D-C can have a resolution of 25 microns.) The PMS 2D-P measured particles from 100 to 3200 microns with a 100 micron resolution.

Microfilm of the processed PMS data shows the images of the particles and gives some statistics of ice mass content, radar reflectivity, concentration and particle size. From the 2 dimensional image, a 3 dimensional volume is assumed. The ice crystals were not separated into habits, so a single density of 0.5 g/cm^3 was used. The counts given in the size bins are not correct, but should be in most cases half the value given. (The sum of the bins is the total accepted particles and the total accepted spherical particles, and since in most cases all the accepted particles were determined to be spherical, the correct number in the size bins is half the value given.) The raw data on tape is also available.

2.2 CSU Instrumentation

The Sabreliner flew with three instruments from CSU--the CSU Multidirectional Photodiode Radiometer, the CSU Scanning Spectral Radiometer, and the Barnes PRT-6 Radiometer.

The CSU Multidirectional Photodiode Radiometer (Davis, et al, 1980), better known as the Bugeye, was mounted on the

underside of the fuselage. It consists of 13 diodes mounted with different nadir and azimuth angles. Table 3 shows the configuration of the bugeye. A zero azimuth points toward the front of the plane and a zero nadir points down normal to the aircraft. Each diode has a 50 degree field of view to cover as much of the hemisphere with a minimum amount of overlap. Filters were placed over the photodiodes to give a spectral response as shown in Figure 2. A 14th photodiode was mounted pointing up normal to the aircraft to measure the down-welling irradiance. A flat ground glass lens gave the upward looking photodiode a 2π steradian field of view. Table 4 shows the zero offsets and the ratio of diode 1 to diode i. To correct the sensor voltages to an equivalent diode 1 voltage (with offset applied) use the equation:

$$\text{Corrected Voltage} = (\text{Raw Voltage} - \text{Offset}) * \text{Ratio. (2)}$$

The CSU Scanning Spectral Radiometer is capable of scanning from nadir to zenith and uses a continuously variable filter wheel to measure the spectrum from 0.3 to 3.5 microns. It also used discrete filters to measure longwave radiation at wavelengths 0.65, 0.85, 1.6, 2.4, 3.7 and 10.3 microns. The radiometer was referenced to to an NBS blackbody standard detector to within 1%. Data was sampled at 250 Hz and stored on streaming tape. The data was also stored by the Sabreliner data collection system at 1 Hz as a backup. This backup can be found on the Sabreliner subset on

Table 3. The angular positions of the bug-eye photodiodes. (Azimuth angle of zero degrees is forward looking and the angles increase in value in the clockwise direction as one faces the bug-eye dome).

Photodiode	Azimuth Angle	Nadir Angle
1	-	0
2	90	30
3	210	30
4	330	30
5	150	45
6	270	45
7	30	45
8	120	60
9	180	60
10	240	60
11	300	60
12	0	60
13	60	60

Table 4. Bug-eye zero offsets and ratios of Photodiode 1 to Photodiode i.

Photodiode	Zero Offset (Volts)	Photodiode 1 / Photodiode i
1	0.0124	1.000
2	0.0167	1.037
3	0.0166	1.208
4	0.0137	1.057
5	0.0138	0.999
6	0.0140	0.989
7	0.0164	1.004
8	0.0195	0.945
9	0.0172	0.969
10	0.0196	1.169
11	0.0166	1.029
12	0.0142	0.992
13	0.0148	0.995
Bugette	0.0074	1.993

BUGEYE SENSITIVITY WITH FILTERS

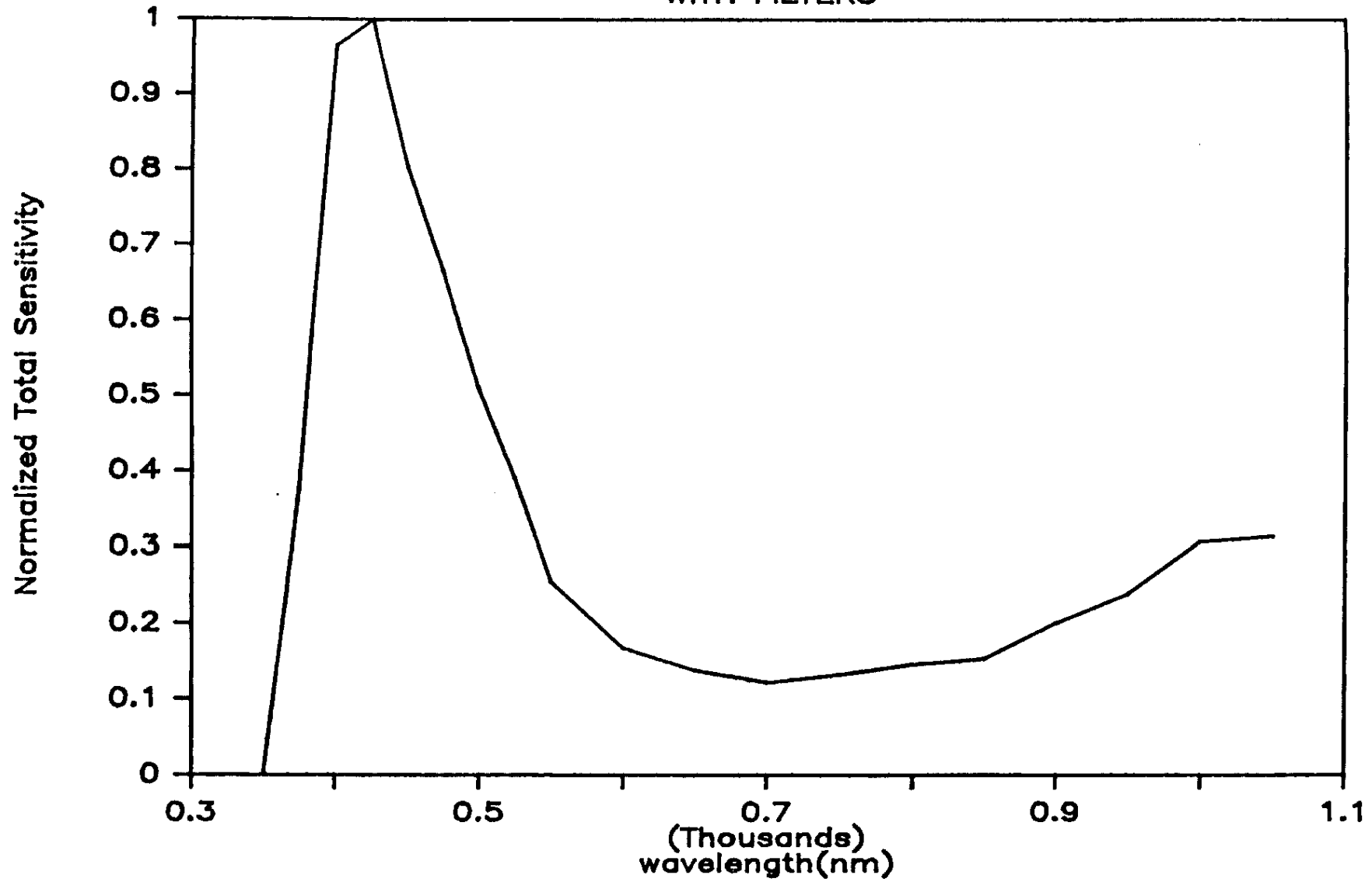


Figure 2. Spectral response of the Bugeye photodiodes.

the streaming tape archive.

The Barnes PRT-6 Radiometer was looking in the horizontal plane of the aircraft with a 14.8 micron bandpass filter to measure air temperature in the manner reported by Albrecht, et al (1979). Data were sampled at 5 Hz and stored as 1 Hz averages by the Sabreliner data collection system. (The data were also stored on Streaming tape as a backup.)

3.0 DATA DESCRIPTION

3.1 Data Accessible From CSU Vax Computer

The data tapes received from NCAR were in a packed 64 bit positive integer form. The data were unpacked (using program UNPAC by $\text{Real} = (\text{Integer-Bias})/\text{Gain}$) and stored on four 6250 bpi tapes in a Vax labeled tape format. The files can be copied to Vax disk using the copy command. The data on the tapes are stored in a (1X,5F12.5) format. Note that the data should be rounded to the first three decimal places. The fact that the last two decimal places may be non-zero arises from Vax numerical inaccuracies. Also altitude data values greater than 9999.999 should be considered accurate to within .002, instead of the .001 figure for other variables; this results from the 7 digit single precision accuracy, $\text{Real}*4$, used in unpacking the data. The tapes, listed below in Table 5, are labeled FIRE x , where x is the tape number. Table 6 lists the variables available.

A Vax program called STRIP is available that will save specified variables in a file to reduce the size of file to work with or to transfer. The size of the header is also reduced, saving only the pertinent information. STRIP will find the start and end times, latitudes, and longitudes as well as the mean altitude of the level portions of the flight. The level portions are determined by using a

Table 5. Files of the Vax labeled tapes.

TAPE:	FIRE1	FIRE2	FIRE2A	FIRE3
F	13OCTF1.DAT ¹	20OCTF2.DAT ²	27OCTF1.DAT	31OCTF1.DAT
I	15OCTF1.DAT	21OCTF1.DAT	27OCTF2.DAT	31OCTF2.DAT
L	15OCTF2.DAT	22OCTF1.DAT	27OCTF3.DAT	02NOVF1.DAT
E	19OCTF1.DAT	22OCTF2.DAT	28OCTF1.DAT	02NOVF2.DAT
	20OCTF1.DAT	24OCTF1.DAT	28OCTF2.DAT	SOUND.HDR ³
N			28OCTF3.DAT	SOUND1.DAT
A			28OCTF4.DAT	SOUND2.DAT
M			30OCTF1.DAT	SOUND3.DAT
E			30OCTF2.DAT	SOUND4.DAT
S				SOUND5.DAT
				SOUND6.DAT
				SOUND7.DAT
				SOUND8.DAT
				SOUND9.DAT
				SOUND10.DAT
				SOUND11.DAT
				SOUND12.DAT
				SOUND13.DAT
				SOUND14.DAT
				SOUND15.DAT
				SOUND16.DAT
				SOUND17.DAT
				SOUND18.DAT
				13OCTF1.DAT

¹13OCTF1.DAT contains a parity error and can not be read, however there is a readable copy at the end of FIRE3.

²20OCTF2.DAT is actually named on tape as 20OCTF1.DAT. When the file is copied from tape to disk it should be done as COPY tapedrive:[0,0]20OCTF1.DAT 20OCTF2.DAT, so the file will then have the correct name.

³The 19 SOUND files, a header file and 18 data files (one for each flight), are a subset of the other files. These files contain the ascent and descent portions of the flights with variables of time, latitude, longitude, pressure, temperature, dew point temperature, wind direction, wind speed, altitude, potential temperature, equivalent potential temperature, absolute humidity, relative humidity, water vapor mixing ratio, and Lyman alpha hygrometer voltage.

Table 6. The variables on Vax tape.

INDEX	VARIABLE	VARIABLE DESCRIPTION	UNITS
1	HR	UNALTERED TAPE TIME	HR
2	MIN	UNALTERED TAPE TIME	MIN
3	SEC	UNALTERED TAPE TIME	S
4	TPTIME	RAW TAPE TIME	S
5	PTIME	PROCESSOR TIME	S
6	TMLAG	ARINC TIME LAG	S
7	ALAT	INS LATITUDE	DEG
8	CLAT	LORAN-C LATITUDE	DEG
9	ALON	INS LONGITUDE	DEG
10	CLON	LORAN-C LONGITUDE	DEG
11	DEI	DISTANCE EAST OF START	KM
12	DNI	DISTANCE NORTH OF START	KM
13	PSFDC	CORRECTED STATIC PRESSURE (FUSELAGE DI)	MB
14	PSFC	CORRECTED STATIC PRESSURE (FUSELAGE)	MB
15	PSBC	CORRECTED STATIC PRESSURE (BOOM)	MB
16	ATF	AMBIENT TEMPERATURE (FUSELAGE)	C
17	ATFH	AMBIENT TEMPERATURE (FUSELAGE HEATED)	C
18	DPTC	DEW POINT TEMPERATURE (THERMOELEC) (TOP)	C
19	DPBC	DEW POINT TEMPERATURE (THERMOELEC) (BOT)	C
20	WD	HORIZONTAL WIND DIRECTION	DEG
21	WS	HORIZONTAL WIND SPEED	M/S
22	UI	WIND EAST COMPONENT	M/S
23	VI	WIND NORTH COMPONENT	M/S
24	WI	WIND VERTICAL COMPONENT	M/S
25	UX	WIND LONGITUDINAL COMPONENT	M/S
26	VY	WIND LATERAL COMPONENT	M/S
27	PALT	NACA PRESSURE ALTITUDE	M
28	HI3	PRESSURE-DAMPED INERTIAL ALTITUDE	M
29	THETA	POTENTIAL TEMPERATURE	K
30	THETAE	EQUIVALENT POTENTIAL TEMPERATURE	K
31	RHODT	ABSOLUTE HUMIDITY (THERMOELEC) (TOP)	G/M3
32	RHODB	ABSOLUTE HUMIDITY (THERMOELEC) (BOT)	G/M3
33	RHUM	RELATIVE HUMIDITY	PCT
34	MR	MIXING RATIO	G/KG
35	SPHUM	SPECIFIC HUMIDITY	G/KG
36	SWT1	TOP S. W. IRRADIANCE, CLEAR DOME, WG295	W/M2
37	SWT2	TOP S. W. IRRADIANCE, RED DOME, WG695	W/M2
38	SWB1	BOT S. W. IRRADIANCE, CLEAR DOME, WG295	W/M2
39	SWB2	BOT S. W. IRRADIANCE, RED DOME, WG695	W/M2
40	IRTC	TOP INFRARED CORRECTED IRRADIANCE	W/M2
41	IRBC	BOTTOM INFRARED CORRECTED IRRADIANCE	W/M2
42	THI	AIRCRAFT TRUE HEADING (ARINC)	DEG
43	THF	AIRCRAFT TRUE HEADING	DEG
44	ALPHA	INS WANDER ANGLE	DEG
45	ROLL	AIRCRAFT ROLL ATTITUDE ANGLE	DEG
46	PITCH	AIRCRAFT PITCH ATTITUDE ANGLE	DEG

Table 6. (Continued)

INDEX	VARIABLE	VARIABLE DESCRIPTION	UNITS
47	ACINS	AIRCRAFT INS ACCELERATION	M/S ²
48	VZI	RAW INS VERTICAL VELOCITY	M/S
49	WP3	DAMPED AIRCRAFT VERTICAL VELOCITY	M/S
50	GSF	INS GROUND SPEED	M/S
51	VEW	INS GROUND SPEED EAST COMPONENT	M/S
52	VNS	INS GROUND SPEED NORTH COMPONENT	M/S
53	XVI	INS GROUND SPEED X COMPONENT	M/S
54	YVI	INS GROUND SPEED Y COMPONENT	M/S
55	TASF	AIRCRAFT TRUE AIRSPEED (FUSELAGE)	M/S
56	TASB	AIRCRAFT TRUE AIRSPEED (BOOM)	M/S
57	QCFC	CORRECTED DYNAMIC PRESSURE (FUSELAGE)	MB
58	QCBC	CORRECTED DYNAMIC PRESSURE (BOOM)	MB
59	QCF	RAW DYNAMIC PRESSURE (FUSELAGE)	MB
60	QCB	RAW DYNAMIC PRESSURE (BOOM)	MB
61	AKDF	ATTACK ANGLE (DIFFERENTIAL PRESSURE)	DEG
62	SSDF	SIDESLIP ANGLE (DIFFERENTIAL PRESSURE)	DEG
63	ADIF	ATTACK DIFFERENTIAL PRESSURE	MB
64	BDIF	SIDESLIP DIFFERENTIAL PRESSURE	MB
65	PSFD	RAW STATIC PRESSURE (FUSELAGE DI)	MB
66	PSF	RAW STATIC PRESSURE (FUSELAGE)	MB
67	PSB	RAW STATIC PRESSURE (BOOM)	MB
68	TTF	TOTAL TEMPERATURE (FUSELAGE)	C
69	TTFH	TOTAL TEMPERATURE (FUSELAGE HEATED)	C
70	DPT	DEW/FROST POINT TEMP (THERMOELEC) (TOP)	C
71	DPB	DEW/FROST POINT TEMP (THERMOELEC) (BOT)	C
72	VLA	RAW LYMAN-ALPHA VOLTAGE	VDC
73	IRT	RAW TOP INFRARED IRRADIANCE	W/M ²
74	IRB	RAW BOTTOM INFRARED IRRADIANCE	W/M ²
75	DTT	TOP PYRGEOMETER DOME TEMPERATURE	C
76	STT	TOP PYRGEOMETER SINK TEMPERATURE	C
77	DTB	BOTTOM PYRGEOMETER DOME TEMPERATURE	C
78	STB	BOTTOM PYRGEOMETER SINK TEMPERATURE	C
79	RICE	RAW ICING RATE INDICATOR	VDC
80	V10	10-V REFERENCE	VDC
81	TADS	AIR TEMP ADS INTERFACE	C
82	FZV	FIXED ZERO VOLTAGE	VDC
83	VDREF	DIFFERENCE OF 10-V REFERENCES	VDC
84	CCEP	LORAN C CIRCULAR ERROR OF PROBABILITY	NMI
85	CGS	LORAN-C GROUND SPEED	M/S
86	POSDF	DIFF. IN POSITION BET. INS & LORAN C	NMI
87	RADSIG	CSU SPECTRAL RADIOMETER SIGNAL	VDC
88	CVFRMP	CSU CVF RAMP SIGNAL	VDC
89	CVFSNC	CSU CVF SYNC PULSE	VDC
90	BBREF	CSU BLACK BODY TEMPERATURE	VDC
91	PRT6	CSU PRT6 RADIOMETER SIGNAL	VDC
92	PRT6BB	CSU PRT6 REFERENCE TEMPERATURE	VDC

Table 6. (Continued)

INDEX	VARIABLE	VARIABLE DESCRIPTION	UNITS
93	BUGETT	CSU UPWARD LOOKING PHOTODIODE	VDC
94	BUG1	CSU BUG EYE CHANNEL 1	VDC
95	BUG2	CSU BUG EYE CHANNEL 2	VDC
96	BUG3	CSU BUG EYE CHANNEL 3	VDC
97	BUG4	CSU BUG EYE CHANNEL 4	VDC
98	BUG5	CSU BUG EYE CHANNEL 5	VDC
99	BUG6	CSU BUG EYE CHANNEL 6	VDC
100	BUG7	CSU BUG EYE CHANNEL 7	VDC
101	BUG8	CSU BUG EYE CHANNEL 8	VDC
102	BUG9	CSU BUG EYE CHANNEL 9	VDC
103	BUG10	CSU BUG EYE CHANNEL 10	VDC
104	BUG11	CSU BUG EYE CHANNEL 11	VDC
105	BUG12	CSU BUG EYE CHANNEL 12	VDC
106	BUG13	CSU BUG EYE CHANNEL 13	VDC

threshold of a change in altitude of 3 meters in a second for two consecutive seconds to determine the start and end times (see Appendix 2). Missing time periods or bad times are also checked for. The header and variables are saved in FOR0nn.DAT, where nn is the given unit number. The information on the level portions is saved in FOR0mm.DAT, where mm=nn+1. Note that I/O unit 2 is reserved for the input. The data is saved in (1X,8F9.3) format. (The blank space in front is lost in an ascii transfer.)

3.2 Data Archived on Streaming Tape

Sixty-four variables of the 106 total were transferred to the Zenith PC and were saved on streaming tape with the filename of C:\DATA\ddmmmFn.DAT, where dd is the day, mmm is the 3 letter month abbreviation (OCT or NOV), and n refers to the nth file for that day. Table 7 is a list of the 64 variables. The "old index" refers to the position of the variable in relation to the total 106 variables. The variables are stored in the format (8F9.3) with a blank line between each second. (There is no blank line between each second for C:\DATA\22OCTF3.DAT.) Note at the end of each file there is at least one non-numeric character, usually a '\$' with an escape sequence. These characters will cause a read error which one should account for in the Fortran read statement. Table 7 lists the variables on the two streaming tape cartridges, containing Sabreliner data from the FIRE

Table 7. Streaming tape variables in order of appearance on tape.

INDEX	VARIABLE	VARIABLE DESCRIPTION	UNITS	OLD INDEX
1	HR	UNALTERED TAPE TIME	HR	1
2	MIN	UNALTERED TAPE TIME	MIN	2
3	SEC	UNALTERED TAPE TIME	S	3
4	ALAT	INS LATITUDE	DEG	7
5	ALON	INS LONGITUDE	DEG	9
6	DEI	DISTANCE EAST OF START	KM	11
7	DNI	DISTANCE NORTH OF START	KM	12
8	PSFC	CORRECTED STATIC PRESSURE (FUSELAGE)	MB	14
9	ATF	AMBIENT TEMPERATURE (FUSELAGE)	C	16
10	ATFH	AMBIENT TEMPERATURE (FUSELAGE HEATED)	C	17
11	DPTC	DEW POINT TEMPERATURE (THERMOELEC) (TOP)	C	18
12	DPBC	DEW POINT TEMPERATURE (THERMOELEC) (BOT)	C	19
13	WD	HORIZONTAL WIND DIRECTION	DEG	20
14	WS	HORIZONTAL WIND SPEED	M/S	21
15	UI	WIND EAST COMPONENT	M/S	22
16	VI	WIND NORTH COMPONENT	M/S	23
17	WI	WIND VERTICAL COMPONENT	M/S	24
18	PALT	NACA PRESSURE ALTITUDE	M	27
19	THETA	POTENTIAL TEMPERATURE	K	29
20	THETAE	EQUIVALENT POTENTIAL TEMPERATURE	K	30
21	RHODT	ABSOLUTE HUMIDITY (THERMOELEC) (TOP)	G/M3	31
22	RHODB	ABSOLUTE HUMIDITY (THERMOELEC) (BOT)	G/M3	32
23	RHUM	RELATIVE HUMIDITY	PCT	33
24	MR	MIXING RATIO	G/KG	34
25	SPHUM	SPECIFIC HUMIDITY	G/KG	35
26	SWT1	TOP S. W. IRRADIANCE, CLEAR DOME, WG295	W/M2	36
27	SWT2	TOP S. W. IRRADIANCE, RED DOME, WG695	W/M2	37
28	SWB1	BOT S. W. IRRADIANCE, CLEAR DOME, WG295	W/M2	38
29	SWB2	BOT S. W. IRRADIANCE, RED DOME, WG695	W/M2	39
30	IRTC	TOP INFRARED CORRECTED IRRADIANCE	W/M2	40
31	IRBC	BOTTOM INFRARED CORRECTED IRRADIANCE	W/M2	41
32	THF	AIRCRAFT TRUE HEADING	DEG	43
33	ROLL	AIRCRAFT ROLL ATTITUDE ANGLE	DEG	45
34	PITCH	AIRCRAFT PITCH ATTITUDE ANGLE	DEG	46
35	GSF	INS GROUND SPEED	M/S	50
36	TASF	AIRCRAFT TRUE AIRSPEED (FUSELAGE)	M/S	55
37	VLA	RAW LYMAN-ALPHA VOLTAGE	VDC	72
38	IRT	RAW TOP INFRARED IRRADIANCE	W/M2	73
39	IRB	RAW BOTTOM INFRARED IRRADIANCE	W/M2	74
40	DTT	TOP PYRGEOMETER DOME TEMPERATURE	C	75
41	STT	TOP PYRGEOMETER SINK TEMPERATURE	C	76
42	DTB	BOTTOM PYRGEOMETER DOME TEMPERATURE	C	77
43	STB	BOTTOM PYRGEOMETER SINK TEMPERATURE	C	78
44	RICE	RAW ICING RATE INDICATOR	VDC	79

Table 7. (Continued)

INDEX	VARIABLE	VARIABLE DESCRIPTION	UNITS	OLD INDEX
45	RADSIG	CSU SPECTRAL RADIOMETER SIGNAL	VDC	87
46	CVFRMP	CSU CVF RAMP SIGNAL	VDC	88
47	CVFSNC	CSU CVF SYNC PULSE	VDC	89
48	BBREF	CSU BLACK BODY TEMPERATURE	VDC	90
49	PRT6	CSU PRT6 RADIOMETER SIGNAL	VDC	91
50	PRT6BB	CSU PRT6 REFERENCE TEMPERATURE	VDC	92
51	BUGETT	CSU UPWARD LOOKING PHOTODIODE	VDC	93
52	BUG1	CSU BUG EYE CHANNEL 1	VDC	94
53	BUG2	CSU BUG EYE CHANNEL 2	VDC	95
54	BUG3	CSU BUG EYE CHANNEL 3	VDC	96
55	BUG4	CSU BUG EYE CHANNEL 4	VDC	97
56	BUG5	CSU BUG EYE CHANNEL 5	VDC	98
57	BUG6	CSU BUG EYE CHANNEL 6	VDC	99
58	BUG7	CSU BUG EYE CHANNEL 7	VDC	100
59	BUG8	CSU BUG EYE CHANNEL 8	VDC	101
60	BUG9	CSU BUG EYE CHANNEL 9	VDC	102
61	BUG10	CSU BUG EYE CHANNEL 10	VDC	103
62	BUG11	CSU BUG EYE CHANNEL 11	VDC	104
63	BUG12	CSU BUG EYE CHANNEL 12	VDC	105
64	BUG13	CSU BUG EYE CHANNEL 13	VDC	106

Cirrus IFO.

3.3 Data Quality

In general, the overall quality of the data from the sabreliner is excellent. The information from this section comes from the Data Quality Report by Griffith (1986), which lists the general limitations and biases in the data and also some (not all) of the isolated problems on a flight-by-flight basis. For a more complete account of the data quality see his report, which can be found with FIRE data package. This report will list the areas of concern as found by Griffith (1986).

1. Two of the three pressure measurements, PSBC and PSFC, are sensitive to rapid temperature changes and can be subject to errors of up to ± 4 mb. The other pressure measurement PSFDC shows no temperature effects and was used for the derived parameters. Unfortunately the streaming tapes contain only the pressure variable PSFC. The difference between this variable and PSFDC is rarely greater than 1 mb and then not much greater.

2. The two airspeed transducers, QCBC and QCFC, show differences of up to ± 1.5 mb when there are large changes in airspeed. The installation of the CSU radiometer and black body caused a slight change in a pressure correction function to correct for the location of the pressure instrument on the aircraft.

3. FM radio transmissions produced interference on several channels. ATF, IRTC, ATFH, DTT, DTB, STT, STB, SWT1 and SWT2 were affected. (And to a very minor extent VLA was affected.) Also derived parameters such as THETA, THETAE and RHUM will show the spikes.

4. The dewpoint sensors, DPTC and DPBC, have a slow response time when compared with the rate of the ascent/descent of the aircraft. This results in erroneous values many times because of lag. The values can be checked against the Lyman-alpha, which was very reliable throughout the experiment. (One can convert the Lyman-alpha voltages to absolute humidity over a short time period by doing a simple point-slope regression on the absolute humidity derived from the slower sensors. The regression line will provide a "steady state".) One should also screen values where the rate of ascent/descent of the aircraft is greater than 1000 meters per minute.

DPTC and DPBC were often pegged at their minimum value at high altitudes. Being pegged caused erroneously high values in the derived humidity variables. DPTC pegged at -54.710 C and DPBC at -54.068 C. One should screen the dew point values and the values of the depended variables if the relative humidity is greater than 100% and if the DPTC and DPBC are near their minimum values. DPTC was used in the derivation of the derived variables because of a better overall performance.

5. The pyranometers (SWT1, SWT2, SWB1 and SWB2) showed temperature effects.

6. The dome/sink temperature difference was used to correct the raw values from the pyrgeometers (IRT and IRB), however recent work by Griffith and Glover (1986) show that there is a significant lag in the dome temperature (DTT and DTB). By taking into account of this lag, the corrected infrared irradiance can be noticeably improved in situations of temperature change such as plane ascents/descents and airspeed changes. The lag correction is not yet used in the post-flight processing of the data.

7. A Loran C navigation system was installed along with the normal INS. In comparing the two systems one sees that the Loran C signal was missing a noticeable fraction of the time and the Loran computed ground speed was slow to adjust to a heading change.

8. The long term average of the computed vertical wind speed was forced to zero. Note that absolute vertical wind speed measurements are still beyond the state of the art. Also the Sabreliner boom is somewhat flexible, effecting the vertical velocity measurements.

9. Wind direction and speed may be in error during steep banking maneuvers and rapid descents.

At the beginning of each spool of microfilm is a list of sensors used in computing the derived parameters. This can be helpful in tracking down problem data. Also calibration maneuvers (for wind measurements) were performed on three of the 18 flights.

REFERENCES

- Albrecht, B. A., S. K. Cox and W. H. Schubert, 1979: Radiometric measurements of in-cloud temperature fluctuations. J. Appl. Meteor., **18**, 1066-1071.
- Baumgardner, D., 1985: Airborne measurements for cloud microphysics. NCAR RAF Bulletin No. 24.
- Griffith, K., 1986: Data quality report. Personal communication.
- Griffith, K. and V. Glover, 1986: Techniques for improving aircraft radiation measurements. NCAR internal report.
- Robinson, N., 1966: Solar radiation. Elsevier Publishing Company. 347pp.
- Starr, D. O'C., 1987: A cirrus-cloud experiment: Intensive field observations planned for FIRE. Bull. Amer. Meteor. Soc., **68**, 119-124.

APPENDIX 1: SABRELINER FLIGHT SUMMARIES

Below is a brief comment on each of the flights extracted from the Sabreliner flight logs. The takeoff and landing times are in Coordinated Universal Time (CUT or GMT).

13OCT86 FLIGHT 1

Takeoff Time: 18:30

Landing Time: 19:33

Locale: Southwestern Wisconsin

This was a short flight due to an aircraft battery malfunction.

15OCT86 FLIGHT 2

Takeoff Time: 18:10

Landing Time: 20:48

Locale: Central Wisconsin

Excellent Bugeye data was seen outside the cirrus bands and during the spiral descent. Satellite overpass at approximately 2000 GMT.

19OCT86 FLIGHT 3

Takeoff Time: 15:16

Landing Time: 17:58

Locale: Western Minnesota

The Sabreliner was flown with the ER-2 above and the King Air below. The aircraft flew through a well defined cirrus band, and the Sabreliner had coincidence with ER-2 above and King Air below at flight levels of 26,000 feet and below.

19OCT86 FLIGHT 4

Takeoff Time: 19:42

Landing Time: 22:27

Locale: Central Minnesota

This flight was a continuation of Flight 3 in the afternoon. (Flight 3 data is considered to be the better of the two.)

20OCT86 FLIGHT 5

Takeoff Time: 14:20

Landing Time: 16:37

Locale: Northern Lake Michigan

This flight was considered a marginal flight because the cirrus quickly dissipated.

21OCT86 FLIGHT 6

Takeoff Time: 16:52

Landing Time: 19:35

Locale: Iowa

In this flight a cell was encountered, "hanging" from a layer above. The Sabreliner was flown over Iowa. There was an interesting haze over southwest Wisconsin on the ferry out. The haze should show strong forward scattering characteristics in the bug-eye data.

22OCT86 FLIGHT 7

Takeoff Time: 13:36

Landing Time: 16:26

Locale: Wausau, Wisconsin

This is an excellent thin cirrus case, upwind from the Wausau lidar. Interesting bug-eye data was taken on the loiter, in the turns and during the ferry to Wausau. The Sabreliner flew over Wausau at flight levels of 35,000, 37,000 and 39,000 feet.

22OCT86 FLIGHT 8

Takeoff Time: 18:09

Landing Time: 20:56

Locale: South Central Wisconsin

The Sabreliner was flown between Oshkosh and Wisconsin Dells, and is an excellent thick, uniform cirrus case.

24OCT86 FLIGHT 9

Takeoff Time: 18:11

Landing Time: 20:49

Locale: Lake Michigan, east of Oshkosh

The Sabreliner flight was coordinated with the ER-2. The Sabreliner was flown above and in a CiSt deck. The flight is a good bug-eye case.

27OCT86 FLIGHT 10

Takeoff Time: 18:09

Landing Time: 20:25

Locale: Northeastern Minnesota

At the start of the flight, the Sabreliner was flown in formation with the King Air at 4500 feet. The flight had poor continuity because the cirrus band dissipated.

27OCT86 FLIGHT 11

Takeoff Time: 22:29

Landing Time: 24:45

Locale: Eastern Minnesota

The Sabreliner was flown at night to find the optical offset values for the pyranometers.

28OCT86 FLIGHT 12

Takeoff Time: 15:08

Landing Time: 17:07

Locale: Lake Michigan, east of Oshkosh

The Sabreliner was coordinated with the Landsat overpass at the point 44° 22' N 87° 30' W at 1553 GMT. A good cirrus layer persisted during the flying of the racetracks. The flight ended early due to radio problems with ATC.

28OCT86 FLIGHT 13

Takeoff Time: 19:00

Landing Time: 21:42

Locale: Lake Michigan, east of Oshkosh

This flight contains an excellent data set (but no PMS 2D-P data). There was significant variation in ice crystal size and type as a function of height. The Sabreliner was flown near Oshkosh and ended the flight with a slow descent.

30OCT86 FLIGHT 14

Takeoff Time: 17:55

Landing Time: 20:52

Locale: Iowa

The first racetrack run was flown with fractional cloud cover of several different cloud types. The second racetrack run was in a thin cirrus deck with clear sky below.

31OCT86 FLIGHT 15

Takeoff Time: 14:13

Landing Time: 16:55

Locale: Southwestern Wisconsin

Flight 15 was an excellent flight. Early in the flight, the ER-2 was overhead, and later the Sabreliner penetrated a layer with generating cells that were producing streamers.

31OCT86 FLIGHT 16

Takeoff Time: 19:13

Landing Time: 22:05

Locale: Northern Wisconsin

The Sabreliner was flown through jet stream cirrus.

02NOV86 FLIGHT 17

Takeoff Time: 15:07

Landing Time: 17:52

Locale: Lake Michigan, east of Oshkosh

There is some excellent bug-eye data from this flight. Early part of the flight was coordinated with the ER-2.

02NOV86 FLIGHT 18

Takeoff Time: 19:27

Landing Time: 21:58

Locale: Southwestern Wisconsin

The Sabreliner sampled some sinking cirrus bands SW of Fort McCoy and did a spiral profile over Fort McCoy. There was a NOAA-9 overpass during the flight at approximately 2000 GMT.